

Src-dependent Tyrosine Phosphorylation of Non-muscle Myosin Heavy Chain-IIA Restricts *Listeria monocytogenes* Cellular Infection

Maria Teresa Almeida^{1,2,3}, Francisco S. Mesquita^{1,2,4}, Rui Cruz^{1,2,3}, Hugo Osório^{1,5}, Rafael Custódio^{1,2}, Cláudia Brito^{1,2,3}, Didier Vingadassalom⁶, Mariana Martins^{1,2}, John M. Leong^{6,§}, David W. Holden⁴, Didier Cabanes^{1,2*} and Sandra Sousa^{1,2*}

¹Instituto de Investigação e Inovação em Saúde, Universidade do Porto, Portugal

²Group of Molecular Microbiology, Instituto de Biologia Molecular e Celular (IBMC), Universidade do Porto, Porto, Portugal.

³Instituto de Ciências Biomédicas Abel Salazar (ICBAS), Universidade do Porto, Porto, Portugal.

⁴MRC, Centre for Molecular Bacteriology and Infection, Imperial College, London, UK.

⁵Institute of Molecular Pathology and Immunology of the University of Porto (IPATIMUP), Porto, Portugal.

⁶Department of Molecular Genetics and Microbiology, University of Massachusetts Medical School, Worcester, MA, USA.

[§]Present address: Sackler School of Graduate Biomedical Sciences, Tufts University School of Medicine, Boston, MA, USA.

Running title: *Src kinase phosphorylates NMHC-IIA upon bacterial infection.*

*To whom correspondence should be addressed: Didier Cabanes or Sandra Sousa, Group of Molecular Microbiology, Instituto de Biologia Molecular e Celular, Rua do Campo Alegre 823, 4150-180 Porto, Portugal; Tel. +351226074907; FAX +351226099157; E-mail: didier@ibmc.up.pt or srsousa@ibmc.up.pt.

Keywords: post-translational modification, phosphotyrosine signaling, Src, myosin, host-pathogen interactions, Gram positive bacteria, non-muscle myosin IIA, intracellular bacterial pathogen, *Listeria monocytogenes*, cellular infection

Background: Non-muscle myosin IIA is involved in force generation, movement and membrane reshaping. Its activity is regulated by phosphorylation of the light chain.

Results: NMHC-IIA head domain is tyrosine phosphorylated by Src and modulates *Listeria* intracellular levels.

Conclusion: Tyrosine phosphorylation of NMHC-IIA affects the outcome of infection.

Significance: This novel post-translational modification of NMHC-IIA possibly affects its functions.

SUMMARY

Bacterial pathogens often interfere with host tyrosine phosphorylation cascades to control host responses and cause infection. Given the role of tyrosine phosphorylation events in different human infections and our previous results showing the activation of the tyrosine kinase Src upon incubation of cells

with *Listeria monocytogenes* (*Lm*), we searched for novel host proteins undergoing tyrosine phosphorylation upon *Lm* infection. We identify the heavy chain of the non-muscle myosin IIA (NMHC-IIA) as being phosphorylated in a specific tyrosine residue in response to *Lm* infection. We characterize this novel post-translational modification event and show that, upon *Lm* infection, Src phosphorylates NMHC-IIA in a previously uncharacterized tyrosine residue (Y158) located in its motor domain near the ATP-binding site. In addition, we found that other intracellular and extracellular bacterial pathogens trigger NMHC-IIA tyrosine phosphorylation. We demonstrate that NMHC-IIA limits intracellular levels of *Lm* and this is dependent on the phosphorylation of Y158. Our data suggest a novel mechanism of regulation of NMHC-IIA activity relying on the phosphorylation of Y158 by Src.

INTRODUCTION

Listeria monocytogenes (*Lm*) is a human intracellular foodborne bacterial pathogen that causes serious disease in immunocompromised individuals. Within the host it finds suitable replication niches in the liver and spleen, disseminates and can reach the central nervous system. In pregnant women, *Lm* targets the fetus, eliciting fetal infection and abortions (1). The ability of *Lm* to cause disease relies on its capacity to invade nonphagocytic cells, replicate therein and spread to the entire organism overcoming the intestinal, blood-brain and fetoplacental barriers (2). Through the expression of bacterial factors *Lm* establishes a crosstalk with host cells favoring the progression of the cellular infection (3). In epithelial cells, *Lm* invasion is mainly driven by the bacterial surface proteins InlA and InlB that bind E-cadherin and c-Met, respectively, at the surface of host cells (4,5). This engagement of host cell receptors triggers tyrosine phosphorylation-mediated signaling, resulting in the local activation of the Arp2/3 complex that initiates actin polymerization at the site of *Lm* attachment (6,7), causing membrane invagination that supports bacterial entry. InlB interaction with the receptor tyrosine kinase c-Met stimulates its auto-phosphorylation, induces the tyrosine phosphorylation and recruitment of adaptor proteins, and the activation of phosphoinositide 3-kinase (PI3K) (5,8,9). Phosphatidylinositol (3,4,5)-triphosphate generated by PI3K accumulates at the cell membrane during *Lm* infection (8) and plays a crucial role in the recruitment of molecules controlling actin polymerization, such as Rac1 and WAVE2 (6,10-12). In turn, InlA binding to E-cadherin induces the activation of Src tyrosine kinase that subsequently phosphorylates cortactin, E-cadherin and the clathrin heavy chain (7,13,14). While cortactin and clathrin tyrosine phosphorylations are critical events for actin polymerization and recruitment at the *Lm* entry site (7,13), E-cadherin phosphorylation leads to its ubiquitination, internalization and further degradation (14). The combined action of these events leads to the internalization the *Lm* into epithelial cells.

In this study we aimed to identify new cellular proteins undergoing tyrosine phosphorylation in response to *Lm* infection and address whether such post-translational

modification would regulate cellular infection. The tyrosine phosphorylated proteins were recovered from *Lm*-infected epithelial cells and subjected to mass spectrometry identification. We identified the non-muscle myosin heavy chain IIA (NMHC-IIA) as one of the enriched tyrosine phosphorylated proteins recovered upon *Lm* infection.

NMHC-IIA is an actin-binding protein with motor and contractile properties, involved in cellular processes requiring force generation, cell movement and membrane reshaping (15). In infection, NMHC-IIA is critical for viral entry (16,17) and supports invasion (18) and dissemination (19) of various bacteria. While the serine/threonine phosphorylation of the regulatory light chain is a well-known mechanism to regulate non-muscle myosin IIA activity (15), our knowledge on the regulation of the heavy chain is limited and NMHC-IIA tyrosine phosphorylation has never been characterized. Here we show that NMHC-IIA undergoes tyrosine phosphorylation in response to several bacterial pathogens. Our data indicate that upon *Lm* cellular infection NMHC-IIA was phosphorylated in tyrosine residue 158 by the host Src kinase. In the presence of blebbistatin, a chemical inhibitor of Myosin II activity, the percentage of cells showing *Lm*-associated actin foci was increased and correlated with higher levels of intracellular *Lm*. In addition, increased numbers of intracellular *Lm* were also found in cells depleted for NMHC-IIA as well as in conditions where NMHC-IIA tyrosine phosphorylation is prevented. These results show the involvement of NMHC-IIA in *Lm* infection and point to the regulatory role of its phosphorylation in tyrosine 158 which could affect NMHC-IIA activity. Our findings describe a novel post-translational modification of NMHC-IIA with important implications in bacterial infection. Taking into account the central role of NMHC-IIA in key cell biology processes, our data also suggest the existence of a new mechanism of NMHC-IIA regulation that could be of critical importance in the canonical functions of non-muscle Myosin IIA.

EXPERIMENTAL PROCEDURES

Bacterial strains and cell lines. *Listeria* and *E. coli* strains were grown aerobically at 37 °C, with shaking, in brain-heart infusion (BHI) and Lysogeny Broth (LB) media, respectively. *Yersinia* was grown aerobically at 26 °C, with shaking, in

LB media. When required antibiotics were added to growth media. Details are provided in Table 1. Caco-2 cells (ATCC HTB-37) were cultivated in MEM with L-glutamine, supplemented with non-essential amino acids, sodium pyruvate, and 20% fetal bovine serum (FBS). HeLa (ATCC CCL-2), HEK293 (ATCC CRL-1573) and COS-7 (ATCC CRL-1651) cells were cultivated in DMEM with glucose (4.5 g/l) and L-glutamine, supplemented with 10% FBS. Cells were maintained at 37 °C in a 5% CO₂-enriched atmosphere. Cell culture media and supplements were from Lonza.

Plasmids, antibodies and reagents. Plasmids used are listed in Table 2. Plasmids GFP-NMHC-IIA-Y158F and GFP-NMHC-IIA-Y190F were generated using GFP-NMHC-IIA-WT from Addgene (20) and the QuickChangeII XL site-directed mutagenesis kit (Agilent Technologies). For NMHC-IIA rescue assays, a plasmid encoding siRNA-resistant GFP-NMHC-IIA-WT transcripts was generated. Oligonucleotide sequences are provided in Table 3. Antibodies are listed in Table 4. F-actin was labeled with Alexa Fluor 647- or 555-conjugated phalloidin (Invitrogen). Chemical inhibitors Y-26732 (Sigma-Aldrich), Blebbistatin and PP1 (Calbiochem) were handled as recommended. FluoSpheres-carboxylate modified microspheres were from Invitrogen (F-8814).

Determination of intracellular bacteria. The levels of intracellular bacteria were determined as described (21). When indicated cells were incubated with serum-free medium containing blebbistatin, PP1 or DMSO. Cells were challenged with pre-washed *Lm* at a multiplicity of infection (MOI) of 50 or with *Yp* (MOI 10) for 60 min, treated with 20 µg/ml gentamicin for 90 min, washed in PBS, lysed with 0.2% Triton X-100 and serial dilutions were plated for CFU counting. For immunofluorescence scoring, cells infected with *Lm* (MOI 50) were treated with 100 µg/ml gentamicin for 10 min, and washed with 20 µg/ml gentamicin prior fixation.

Immunoprecipitation assays. HeLa or Caco-2 cells grown until confluence were washed twice with warm phosphate-buffered saline (PBS), serum-starved (5 h) and left non-infected (NI) or incubated with pre-washed *Lm* (21) at MOI 200 for different periods of time, or with *E. coli* (EPEC, EHEC or K12-*inv* strains) at MOI 200 for 4 h as described (22). When indicated, cells were treated with 10 µM PP1 or 50 µM Y-27632 30 min before

infection. After washing twice with ice-cold PBS, cells were lysed in 1 ml of lysis buffer [1% Igepal CA-630 (Sigma-Aldrich), 50 mM Tris pH 7.5, 150 mM NaCl, 2 mM EDTA, 1 mM AEBSF (Interchim), PhosSTOP and cOmplete Protease Inhibitor Cocktail (Roche Pharmaceuticals)] and lysates recovered after centrifugation (15,000 × g, 15 min, 4 °C). Cell lysates (500 µg) were incubated overnight (4 °C) with 1 µg of anti-phosphotyrosine 4G10 or 5 µg of anti-NMHC-IIA antibodies. Immune complexes were captured with 50 µl of PureProteome Protein A or G magnetic beads (Millipore). Immunoprecipitated fractions were resolved by SDS-PAGE and gels were silver-stained using the ProteoSilverTM Plus Silver Staining Kit (Sigma-Aldrich) or processed for immunoblotting. For kinase assay, HEK293 cells were harvested and lysed 24 h post-transfection, GFP fusion proteins were immunoprecipitated with anti-GFP conjugated agarose beads (sc-9996 AC, Santa Cruz Biotechnology) and eluted in 0.2 M glycine, pH 2.5.

Protein identification by mass spectrometry (MS). Protein identification was performed by MALDI TOF/TOF mass spectrometry as described (23). Protein bands were excised from SDS-PAGE gels, reduced with dithiothreitol, alkylated with iodoacetamide and in gel digested with trypsin. Peptides were extracted, desalted, concentrated using ZipTips (Millipore), crystallized onto a MALDI sample plate and analyzed using a 4700 Proteomics Analyzer MALDI-TOF/TOF (Applied Biosystems). Peptidic mass spectra were acquired in reflector positive mode at a 700-4000 m/z mass window and proteins identified by Peptide Mass Fingerprint using the Mascot software (Matrix Science, UK) integrated in the GPS Explorer software (ABSCIEX, CA) and searched against the SwissProt/UniProt *Homo sapiens* protein sequence database. The maximum error tolerance was 35 ppm and up to two missed cleavages were allowed.

Phosphopeptide analysis by MS. Bands corresponding to NMHC-IIA, from anti-NMHC-IIA IPs of NI and *Lm*-infected HeLa cells, were processed as described above. Phosphopeptides were selectively enriched by titanium dioxide chromatography (TiO₂ Mag Sepharose, GE Healthcare). MALDI matrix used was THAP/DAC (2',4',6'-trihydroxyacetophenone monohydrate 9 mg/mL, diammonium citrate 5 mg/mL, in water/Acetonitrile 50:50, v/v). Mass spectra were

acquired in a 4800 Plus MALDI TOF/TOF Analyzer mass spectrometer (AB SCIEX) both in reflector negative and MS/MS modes.

Immunoblotting. Proteins were resolved in SDS-PAGE gels and transferred onto Nitrocellulose membranes (Hybond ECL, GE Healthcare Life Sciences). Membranes were blocked with 5% skimmed milk in buffer A (150 mM NaCl, 20 mM Tris-HCl pH 7.4 and 0.1% Triton X-100) for 1 h at room temperature or overnight at 4°C. Primary and secondary antibodies were diluted in 2.5% skimmed milk in buffer A. Membranes used for anti-phosphotyrosine detection were blocked with Western Blocker solution (Sigma Aldrich), also used to dilute primary and secondary antibodies.

Immunofluorescence analysis. Cells were fixed in 3% paraformaldehyde (15 min), quenched with 20 mM NH₄Cl (1 h), permeabilized with 0.1% Triton X-100 (5 min) and blocked with 1% BSA in PBS (30 min). Antibodies were diluted in PBS containing 1% BSA. Coverslips were incubated 1 h with primary antibodies washed three times in PBS and incubated 45 min with secondary antibodies and Phalloidin Alexa-555 or 647. DNA was counterstained with DAPI (Sigma-Aldrich). Coverslips were mounted onto microscope slides with Aqua-Poly/Mount (18606, Polysciences). Images were collected with a confocal laser-scanning microscope (Zeiss Axiovert LSM 510 or Leica SP2 AOBSE) and processed using Adobe Photoshop software.

Transfection and lentiviral transduction. The lentiviral shRNA expression plasmids Mission pLKO.1-puro (control) and Mission shRNA-cSrc (Sigma-Aldrich), were used in combination with the envelope plasmid pMD.G, and packaging plasmid pCMVR8.91. Packaging, envelope, and shRNA vector plasmids were co-transfected into HEK293 cells. Viral supernatants harvested after 72 h, filtered and incubated with target HeLa cells for 48 h at 37°C. Puromycin was used to select for individual clones. The knock-down verified by immunoblot and/or real-time RT-PCR.

Transfection of siRNA duplexes and plasmid DNA. HeLa cells seeded in 24- or 6-well plates were transfected with 60 nM of control siRNA-D (sc-44232 Santa Cruz Biotechnology) or specific siRNAs for NMHC-IIA or NMHC-IIB depletion, using Lipofectamine RNAiMax (Invitrogen) following manufacturer's instructions. Assays

were performed 48 h later. Sequences of siRNAs are provided in Table 4. For transient protein expression, HeLa cells were seeded in 24-well plates (1x10⁵ cells/well), 6-well plates (4x10⁵ cells/well), or 10 cm dishes (3x10⁶ cells/dish), and transfected at 90% confluency with 500 ng, 2.5 µg or 15 µg of plasmid DNA, respectively, using Lipofectamine 2000 (Invitrogen). Assays were performed 24 h later. For rescue assays, HeLa cells were transfected with NMHC-IIA-si#2 and 24 h later transiently transfected with plasmids encoding siRNA-resistant GFP-NMHC-IIA-WT.

Kinase Assay. Kinase assays were performed using the Src Assay Kit (17-131, Millipore), following manufacturer's instructions. Anti-GFP-immunoprecipitated fractions from HEK293 cells expressing GFP-NMHC-IIA variants were incubated (10 min, 30 °C) with 10 units of recombinant Src (14-117, Millipore), in 30 µl of kinase reaction buffer supplemented with 9 µl of Manganese/ATP Cocktail and 10 µCi γ ³²P-ATP (PerkinElmer). Reactions including a Src-specific substrate or lacking Src were used as controls. Reactions were precipitated with 40% TCA and spotted onto P81 phosphocellulose paper squares, washed three times with 0.75% phosphoric acid, once with acetone and transferred to microtubes containing UniverSol liquid scintillation cocktail (MP Biomedicals). Incorporation of ³²P was determined in a Wallac 1450 MicroBeta TriLux liquid scintillation counter (PerkinElmer), as counts per minute (cpm). Radioactivity measurements were performed in duplicate in two independent assays.

Statistical analyses. Statistical analyses were performed with Prism 6 software (GraphPad Software, Inc.). One-way ANOVA with post hoc testing analyses were used for pair-wise comparison of means from at least three unmatched groups. Two-tailed Student's t-test was used to compare means of two samples and one-sample t-test to compare with samples arbitrarily fixed to 100. Differences were not considered statistically significant for *p* value ≥ 0.05.

RESULTS

NMHC-IIA is tyrosine-phosphorylated in response to bacterial infection. To identify new host proteins undergoing tyrosine phosphorylation (pTyr) in response to *Lm* and which could affect *Lm* cellular infection, we compared the pTyr

protein profiles of *Lm*-infected and non-infected (NI) HeLa cells. Cell extracts were collected at different time points post inoculation and subjected to immunoprecipitation (IP) using anti-phosphotyrosine antibodies (anti-pTyr). IP fractions were resolved by SDS-PAGE followed by silver staining. Bands showing variable intensities in *Lm*-infected versus NI cells were excised and processed for mass spectrometry identification. A band corresponding to a ≈ 250 kDa protein and displaying increased intensity throughout the infection (Fig. 1A) was identified as the human non-muscle myosin heavy chain IIA (NMHC-IIA) (data not shown).

To validate this result, HeLa and Caco-2 cells were incubated with *Lm* for different time periods and the presence of NMHC-IIA in anti-pTyr IP fractions was assessed by immunoblot using NMHC-IIA specific antibodies. We detected a time-dependent increase of NMHC-IIA in IP fractions from *Lm*-infected cells (Fig. 1B). Levels of NMHC-IIA in pTyr fraction increased 3.5-fold after 60 minutes of *Lm* incubation with HeLa cells and 15-fold in Caco-2 cells upon 20 minutes of *Lm* infection (Fig. 1B). Levels of NMHC-IIA in whole cell lysates (WCL) were not affected by infection (Fig. 1B), showing that increased levels of NMHC-IIA in IP samples are not related to an augmentation of NMHC-IIA expression. Incubation of HeLa cells with the non-pathogenic species *Listeria innocua* (*Li*) for 60 minutes only induced a small enrichment of NMHC-IIA in the anti-pTyr IP fractions as compared to *Lm* (Fig. 1C). In addition, NMHC-IIA was barely detected in IP fractions from HeLa cells stimulated by *E. coli* DH5 α or latex beads (Fig. 1C). Altogether, these results indicate that the enrichment of NMHC-IIA in the pool of pTyr proteins is associated to the pathogenic features of *Lm* and is not a broad cellular response to any extracellular stimuli.

To investigate whether the same response could be induced upon infection with other human bacterial pathogens, HeLa cells were incubated for 4 h with: the extracellular pathogenic *E. coli* EPEC and EHEC; or the invasive *E. coli* K12 expressing the *Yersinia pseudotuberculosis* (*Yp*) invasin (K12-*inv*) (24), an infection model allowing the study of signaling pathways triggered downstream the invasin-integrin interaction. As compared to NI conditions, NMHC-IIA appeared slightly increased

in anti-pTyr IP fractions from EPEC- and EHEC-infected cells. Strikingly, K12-*inv* induced a robust enrichment of NMHC-IIA in IP samples that is abolished in cells incubated with bacteria harboring a disrupted invasin-encoding gene (K12- Δ *inv*, Fig. 1D). For comparison cells were also incubated with *Lm* for 1 and 4 h (Fig. 1D). These results indicate that the enrichment of NMHC-IIA in the pool of pTyr proteins is an event triggered by several human bacterial pathogens.

Our data suggest that bacterial infection either induces the direct NMHC-IIA pTyr or stimulates its interaction with a protein that undergoes itself pTyr. To address this issue, endogenous NMHC-IIA was immunoprecipitated from NI and *Lm*-infected HeLa cells and pTyr proteins were detected by immunoblot. A band showing a consistent 1.5-fold increase in intensity in infected samples was detected at the molecular weight of NMHC-IIA (Fig. 1E). Immunoprecipitated levels of NMHC-IIA were similar in NI and *Lm*-infected cells. These results support a direct pTyr of NMHC-IIA triggered by *Lm* infection.

NMHC-IIA-pTyr induced by Lm cellular infection requires the activity of Src tyrosine kinase. Considering our previous findings revealing the key role of the tyrosine kinase Src during *Lm* invasion (7), we addressed the role of this kinase in NMHC-IIA-pTyr in the context of *Lm* infection. Prior to *Lm* incubation, HeLa cells were treated with PP1, an inhibitor of Src family kinases, or with Y-27632, an inhibitor of the serine/threonine kinase ROCK that regulates NMHC-IIA activity through the phosphorylation of the regulatory light chain of myosin II and limits *Lm* internalization (25). Given that NMHC-IIA-pTyr is hardly detected by using anti-pTyr antibodies in immunoblot, cell lysates were subjected to anti-pTyr IP assay and NMHC-IIA was detected in IP fractions. The increase in NMHC-IIA-pTyr induced by *Lm* infection of non-treated cells (NT) was abolished in PP1-treated cells while being not affected by Y-27632 treatment (Fig. 2A), suggesting that NMHC-IIA-pTyr requires Src kinase activity and occurs independently from ROCK activity. In addition, we interfered with Src activity by overexpressing a Src kinase-dead variant (Src-KD) (26). Levels of NMHC-IIA-pTyr induced by *Lm* infection were assessed in HeLa cells non-transfected (NT),

transfected with an empty plasmid (Ctr) or overexpressing Src-KD. In contrast to NT and Ctr cells showing increased levels of NMHC-IIA-pTyr upon *Lm* infection, in cells overexpressing Src-KD the NMHC-IIA-pTyr was almost undetectable (Fig. 2B). To further confirm these data, we targeted the expression of endogenous Src by using specific shRNAs. We observed that, *Lm*-induced NMHC-IIA-pTyr occurred in shRNA control (sh Ctr) and was clearly diminished in shRNA Src expressing (sh Src) HeLa cells, in which Src expression is reduced by 60% (Fig. 2C and 2D). Altogether, these data demonstrate that Src activity is required for NMHC-IIA-pTyr triggered by bacterial infection.

Host Src kinase phosphorylates NMHC-IIA in tyrosine residue 158. The NMHC-IIA amino acid sequence includes 34 tyrosine residues, most of which located in the myosin motor domain (Fig. 3A). To identify the NMHC-IIA tyrosine residues phosphorylated by Src upon *Lm* infection, we used combined *in silico* approaches (NetPhos 2.0 and NetPhosK). Nine tyrosine residues were predicted as potentially phosphorylated, among which only the tyrosine in position 158 (Y158) was a putative substrate for Src kinase (Fig. 3B). To assess these *in silico* predictions and taking into account that *Lm*-induced NMHC-IIA-pTyr requires Src kinase activity (Fig. 2), we determined if NMHC-IIA-pTyr occurs upon *Lm* infection of cells ectopically expressing either GFP-tagged NMHC-IIA-Y158F (in which Y158 residue was replaced by a phenylalanine), NMHC-IIA-Y190F (harboring the same amino acid substitution in position 190, randomly selected and unrelated to *in silico* predictions) or NMHC-IIA-WT (wild type NMHC-IIA). *Lm* infection of non-transfected (NT), NMHC-IIA-WT- and NMHC-IIA-Y190F-overexpressing cells generated increased levels of NMHC-IIA-pTyr as compared to NI cells, while the overexpression of NMHC-IIA-Y158F largely limited *Lm*-induced NMHC-IIA-pTyr (Fig. 3C). Exogenous NMHC-IIA-WT and NMHC-IIA-Y190F were occasionally detected in anti-pTyr IP fractions of *Lm*-infected cells (data not shown). Levels of endogenous NMHC-IIA were comparable in the different conditions and GFP fusion proteins were expressed similarly in NI and infected cells (Fig. 3C). These results corroborate *in silico* predictions and suggest the central role of

Y158 in NMHC-IIA-pTyr triggered upon infection. To validate our results, total lysates from NI and *Lm*-infected cells were probed with an antibody raised against a peptide comprising phosphorylated Y158 residue of NMHC-IIA (pY158). In agreement with our data, levels of NMHC-IIA-pY158 were 1.5-fold increased in *Lm*-infected cells (Fig. 3D). In addition, samples enriched in NMHC-IIA phosphopeptides from NI and *Lm*-infected cells were analyzed by mass spectrometry. A phosphopeptide spanning Y158 (amino acid 142 to 165, KRHEMPPHIYAITDTAYRSMQDR) was detected at m/z 3025.37 [M-H]⁻ (Fig. 3E, cluster I) and at 3041.36 [M-H]⁻ with an oxidized methionine (Fig. 3E, cluster II). In infected samples, the area of cluster I that is correlated with the abundance of the corresponding phosphopeptide, was 4.8-fold increased. Cluster II appeared 2.1-fold more abundant in *Lm*-infected samples as compared to NI. Cluster I was further characterized and validated by MS/MS sequencing. Altogether our data show that phosphorylation occurs in position Y158.

We further evaluate whether NMHC-IIA-pTyr occurs specifically on Y158 through Src activity, performing an *in vitro* kinase assay. GFP-NMHC-IIA-WT or Y158F ectopically expressed in HEK293 cells were highly enriched through immunoprecipitation using an anti-GFP antibody and incubated with purified Src kinase and γ -³²P-ATP. A synthetic peptide substrate for Src was used as positive control. In the absence of kinase, the control peptide (Ctr) and IP fractions of NMHC-IIA-WT and Y158F showed residual levels of γ -³²P-ATP incorporation. In the presence of Src kinase, the NMHC-IIA-WT enriched IP fraction and the control peptide became radiolabeled while the radioactivity incorporation in the NMHC-IIA-Y158F enriched sample remained at a basal level (Fig. 3F).

Altogether these results strongly suggest that Y158 of NMHC-IIA is a substrate for Src kinase, becoming phosphorylated in response to *Lm* infection, and put forward the putative role of this event in cellular infection. In addition, Y158 appears extremely conserved among species ranging from *Saccharomyces cerevisiae* to *Homo sapiens* (Fig. 3G), pointing the broad importance for Y158 in the regulation of highly conserved canonical functions of NMHC-IIA.

Inhibition of NMHC-IIA activity affects intracellular levels of Lm. To assess the role of NMHC-IIA activity in cellular infection, we measured intracellular levels of *Lm* following chemical inhibition of NMHC-IIA. Blebbistatin (Blebb), a specific inhibitor of myosin II activity (27), was added (10 or 100 μ M) to HeLa and Caco-2 cells and *Lm* infection efficiency was quantified by gentamicin protection assays. As control we used an inactive form of blebbistatin [(+)-Blebb]. *Lm* intracellular levels were increased by 2- to 8-fold, in a dose-dependent manner in both cell lines, following treatment with the active [(-)-Blebb] as compared to the inactive enantiomer of blebbistatin (Fig. 4A). Untreated and inactive blebbistatin-treated cells showed similar levels of intracellular *Lm* (data not shown). Our data are in agreement with a previous report showing that blebbistatin treatment of L2 cells increases *Lm* adhesion and invasion (25). Recruitment of NMHC-IIA and formation of actin foci at *Lm* entry sites were both detected in control (DMSO) and active blebbistatin-treated (Blebb) HeLa cells (Fig. 4B). While the percentage of *Lm*-associated cells remained similar in both conditions, the percentage of cells showing *Lm*-actin foci increased in the presence of active blebbistatin (Fig. 4C). Together, our results indicate that the ATPase activity of NMHC-IIA is not required for its localization to the sites of *Lm* uptake and does not influence the interaction of *Lm* with host cells. However, inhibition of NMHC-IIA ATPase activity fosters the formation of *Lm*-actin foci, which correlates with increased rates of intracellular bacteria.

Reduced expression of NMHC-IIA increases the level of intracellular Lm. To further address the role of NMHC-IIA in *Lm* cellular infection, levels of adherent and intracellular *Lm* were quantified by gentamicin protection assays in NMHC-IIA-depleted HeLa cells, using two siRNAs (si#1 and si#2). In accordance with data described above, levels of intracellular *Lm* increased 2-fold in NMHC-IIA-depleted (IIA-si#1 and IIA-si#2) as compared to control siRNA-transfected cells (Ctr) (Fig. 5A). NMHC-IIA depletion assessed by immunoblot reached 85% in si#1-transfected cells and 65% when using si#2 (Fig. 5A). Levels of adhered *Lm* were also augmented in NMHC-IIA-depleted cells (data not shown).

Immunofluorescence analysis of *Lm*-infected NMHC-IIA-depleted cells revealed a 2-fold increase in the percentage of cells associated to *Lm* and a 3-fold increase in the percentage of cells showing *Lm*-associated actin foci (Fig. 5B). The number of bacteria and actin foci per cell were also increased in NMHC-IIA-depleted cells (Fig. 5C), correlating with increased levels of intracellular bacteria. Our data indicate that, while *Lm* association to cells does not require NMHC-II activity it is modulated by NMHC-IIA itself probably through the interaction with other proteins.

To discard the hypothesis that increased levels of intracellular *Lm* detected in NMHC-IIA-depleted cells could result from the overexpression of the isoform B of non-muscle myosin heavy chain (NMHC-IIB), we confirmed that expression levels of NMHC-IIB were similar in NMHC-IIA-depleted cells and control cells (Fig. 5D). In addition, we found that *Lm* intracellular levels decreased 3-fold in NMHC-IIB-depleted HeLa cells (Fig. 5E), suggesting that NMHC-IIA and IIB play opposite roles in *Lm* infection and thus undermining the possibility of their mutual functional replacement. To definitively reinforce our findings and exclude potential uncontrolled off-target effects, we performed gentamicin protection assays following gene rescue experiments. We created a siRNA-resistant GFP-NMHC-IIA construct (NMHC-IIA-siRes) by introducing silent point mutations within the si#2 target sequence. We found that increased levels of intracellular *Lm* detected upon NMHC-IIA depletion (IIA-si#2) dropped to control levels in NMHC-IIA-depleted cells expressing NMHC-IIA-siRes (Fig. 5F). In contrast, the expression of NMHC-IIA-WT in NMHC-IIA-depleted cells did not restore control levels of intracellular *Lm*. Immunoblot analysis confirmed that the expression of endogenous NMHC-IIA was diminished in the presence of si#2 and that ectopically expressed NMHC-IIA was only detected in NMHC-IIA-siRes-transfected cells (Fig. 5F). However, in absence of si#2, both NMHC-IIA-WT and siRes variants are expressed at similar levels (Fig. 5G). Together these results confirm that the increase in *Lm* intracellular levels observed in NMHC-IIA-depleted cells is specifically due to NMHC-IIA depletion.

To analyze whether the role of NMHC-IIA on

intracellular levels of bacteria was specific for *Lm* or could be broadened to other bacterial infectious processes, we performed gentamicin protection assays using *Li* expressing InlB (*Li-inlB*), the major internalin driving *Lm* entry in HeLa cells (28); K12-*inv* and *Yp*. Numbers of intracellular *Li-inlB* were not significantly different in NMHC-IIA-depleted and Ctr cells (Fig. 5H). In contrast, levels of intracellular K12-*inv* and *Yp* were significantly lower in NMHC-IIA-depleted cells (Fig. 5H). Our data indicate that NMHC-IIA is specifically triggered by pathogenic *Lm* and is independent of an InlB-mediated uptake. By the contrary, the invasin-mediated uptake requires NMHC-IIA. Interestingly, NMHC-IIA and IIB were shown to be required for SopB-mediated invasion of *Salmonella* (18). Our findings, together with published reports, reveal that NMHC-IIA plays opposite roles in different infection models: while it is required for an utmost *Yp* and *Salmonella* infection, it has a restrictive role in *Lm* cellular infection.

The function of NMHC-IIA in *Lm* infection relies on the phosphorylation of its tyrosine 158. We reported above two important observations: 1) NMHC-IIA is tyrosine phosphorylated by Src kinase upon *Lm* incubation with cells, and 2) *Lm* intracellular levels are increased in conditions of NMHC-IIA depletion or inhibition of its activity, demonstrating that NMHC-IIA activity limits *Lm* infection. To investigate whether both findings could be interconnected we evaluated levels of intracellular bacteria under conditions where NMHC-IIA-pTyr does not occur. We used cells with compromised Src activity (PP1 treatment and Src-KD overexpression) and cells expressing an NMHC-IIA non-phosphorylatable variant (NMHC-IIA-Y158F). Levels of intracellular *Lm* showed a 2.5-fold increase in PP1-treated HeLa cells as compared to control DMSO-treated cells (Fig. 6A). In agreement, we observed an increase in *Lm* intracellular levels in cells expressing Src-KD (Fig. 6B). Inversely, intracellular levels of K12-*inv* decreased 2-fold in PP1-treated cells (Fig. 6C), as previously reported (29). Increased levels of intracellular *Lm* detected in conditions of Src inactivation and thus in absence of NMHC-IIA-pTyr, correlates with our data showing that reduced levels or inactivation of NMHC-IIA resulted in increased numbers of intracellular *Lm*.

Our data also suggest an association between the role of NMHC-IIA in *Yp* invasin-mediated uptake and invasin-triggered NMHC-IIA-pTyr.

To further confirm the role of NMHC-IIA-pTyr in the *Lm* cellular infection, we evaluated intracellular levels of *Lm* in HeLa and COS-7 cells transiently expressing either the GFP-NMHC-IIA-WT (WT) or the non-phosphorylatable variant GFP-NMHC-IIA-Y158F (Y158F). Contrarily to HeLa cells, COS-7 cells naturally lack NMHC-IIA expression, therefore allowing the overcoming of effects from the endogenous protein. Equivalent expression levels of both constructs were verified by flow cytometry and immunoblot (data not shown). *Lm* intracellular rates were determined by gentamicin protection assays in cell populations containing about 50% of transfected cells. As compared to NMHC-IIA-WT, the expression of NMHC-IIA-Y158F led to increased levels of intracellular *Lm* in both cell lines (Fig. 6D). Thus, NMHC-IIA-Y158F expression recapitulates the increase of intracellular *Lm* in NMHC-IIA-depleted or inactivated cells. Furthermore, both GFP-NMHC-IIA-WT and GFP-NMHC-IIA-Y158F showed the same localization and accumulate at the site of *Lm* entry in HeLa cells (Fig. 6E). These results indicate that, whereas NMHC-IIA subcellular localization and recruitment to the site of bacterial uptake are unrelated to Y158, the phosphorylation of this specific NMHC-IIA tyrosine plays a key role in restraining *Lm* infection.

DISCUSSION

Pathogens interfere with host phosphorylation cascades to foster adhesion, invasion and intracellular survival. Here, we searched for new host proteins undergoing tyrosine phosphorylation upon *Lm* infection. We showed that NMHC-IIA is tyrosine phosphorylated in response to *Lm* as well as to other human bacterial pathogens such as EPEC, EHEC and K12-*inv*. In *Lm* infection, this previously unknown tyrosine phosphorylation event is triggered by Src kinase on residue Y158 of NMHC-IIA, and limits intracellular bacterial levels.

Myosin II activity is regulated by phosphorylation events in serine and threonine residues of the regulatory light chain (15). NMHC-IIA also undergoes serine and threonine phosphorylations, which regulate the assembly of

myosin II filaments *in vitro* and are thought to control subcellular localization of NMHC-IIA and contractility that depends on the actin-crosslinking activity of NMHC-IIA (15). While NMHC-IIA was detected in studies aiming to unravel the global phosphotyrosine signaling in cancer tissues (30,31), its tyrosine phosphorylation has never been characterized. Our data constitutes the first report showing and characterizing NMHC-IIA-pTyr. Our preliminary *in silico* analysis suggest an important and broad role for NMHC-IIA pTyr in position 158: 1) Y158 is highly conserved among species ranging from *Saccharomyces cerevisiae* to *Homo sapiens*, 2) an *in silico* study suggested that the residue Y163 of muscle myosin heavy chain (matching Y158 in NMHC-IIA) could be phosphorylated (32), 3) Y158 is located in the motor domain of NMHC-IIA nearby the ATP-binding pocket and 4) analysis of the crystal structure of myosin motor domain (33) showed that Y158 is exposed at the surface of the protein and is thus accessible for phosphorylation. Thus, we hypothesize that the phosphorylation of NMHC-IIA Y158 could modulate NMHC-IIA activity most probably by affecting its ability to bind and/or hydrolyze ATP. However at this point any other mechanism could be envisaged. In addition it is likely that NMHC-IIA-pTyr in Y158 occurs in specific physiological conditions engaging NMHC-IIA activity and thus plays a role in the regulation of the highly conserved canonical functions of NMHC-IIA. The functional and structural outcomes of such modification are now critical to elucidate.

Our data suggest that, upon infection, only a small pool of NMHC-IIA becomes phosphorylated in Y158, probably concentrated in a restricted subcellular localization and/or interacting with specific partners, which would impact infection. Yet, we observed that both NMHC-IIA-WT and Y158F concentrated around bacteria at the entry site. We also found that phosphorylation of Y158 does not affect the phosphorylation of the myosin regulatory light chain (our unpublished data), that is achieved by MLCK and is required for activation of myosin II motor activity (15). Interestingly, Src was previously shown recruited to membrane blebs where it associates with MLCK and myosin II (34,35). In response to cell swelling, Src and MLCK form a complex in which Src activates MLCK and both regulate a compensatory

membrane retrieval that requires myosin II (35). It is thus conceivable that Src and MLCK could work together to fine-tune the activity of myosin II in the context of infection.

Myosin II isoforms were recently involved in viral and bacterial infections either promoting or limiting pathogen progression. However their role in such processes is still mainly descriptive. NMHC-IIA is required for KSHV and HSV1 entry into cells (16,17,36), facilitates *Salmonella* invasion and regulates its intracellular growth (18,37) and promotes *Chlamydia* dissemination (19). Conversely, myosin II limits bacterial cell-to-cell spread by restraining *Lm* protrusion formation (38) and participating in the formation of *Shigella*-associated septin cages (39). NMHC-IIB is involved in the formation of actin-rich structures that accumulate near the *Salmonella*-containing vacuole and restrain bacterial intracellular multiplication (40). Altogether, these data suggest that the different outcomes associated with myosin II function during infection are probably related to the cellular machinery engaged in the various infectious processes. Our results indicate that NMHC-IIA activity limits *Lm* infection most probably hindering cellular invasion by interfering with the formation of *Lm*-induced actin foci. NMHC-IIA-depleted or inactivated cells were reported to lose cytoplasm cohesion and show increased membrane activity and plasticity (41,42). These phenotypes could thus suggest that the increased numbers of intracellular *Lm* observed in such cells would be greatly due to the disruption membrane rigidity. However, if this was the case, cells displaying low NMHC-IIA activity should be more permissive to any extracellular pathogen, which was not observed in KSHV (17), HSV1 (16) and *Salmonella* (18) infections. In addition, we show here that NMHC-IIA sustains invasion-mediated *Yp* infection and the invasion rate of *Li* expressing InlB was not significantly increased by NMHC-IIA-depletion, thus excluding a non-specific cell invasion mechanism.

NMHC-IIA participates in cellular processes associated to phosphotyrosine signaling, which are largely usurped by bacteria, namely *Lm* and *Yp* (43), during infection. It 1) regulates protrusion formation and cell migration through the generation of actin retrograde flow (44,45), 2) is required for integrin-mediated adhesion maturation (46), 3) controls cell-cell adhesion promoting E-

cadherin clustering and stabilizing cellular junctions (47), and 4) it governs the polarization of epithelial cells generating forces to maintain the epithelia (48). Whether NMHC-IIA is pTyr in these processes is unknown.

In intercellular junctions, NMHC-IIA is critical for the E-cadherin localization (47) and Src activation is required for actin polymerization at cell-cell contacts (49), as it is during E-cadherin-mediated *Lm* invasion (7). Interestingly, Src activation and recruitment of c-Cbl are key events to control c-Met signaling (50). Our data show that Src activity restricts intracellular levels of *Lm* in HeLa cells in which *Lm* uptake is mainly mediated by c-Met and rise the hypothesis that Src is acting through the tyrosine phosphorylation of NMHC-IIA to inhibit entry. Remarkably, in KSHV infection, which depends on integrin and Src activation (51), NMHC-IIA interacts with the ubiquitin ligase c-Cbl (17). The complex c-Cbl-NMHC-IIA associates with the receptor tyrosine kinase EphA2 that amplifies Src signaling to promote viral macropinocytosis (36). It is thus possible that c-Cbl, which is required for *Lm* infection (52), associates with NMHC-IIA and c-Met to modulate *Lm* infection through tyrosine phosphorylation events. To invade cells, *Yp* binds β 1-integrin (53), which *via* its cytoplasmic tail interacts with NMHC-IIA to regulate cell migration (54). As in adhesion and cell migration processes (55), during *Yp* infection the engagement of β 1-integrin leads to the activation of Src kinase (56) that could also act on NMHC-IIA triggering its tyrosine phosphorylation at the site of bacterial attachment thereby promoting *Yp* infection.

Our data open new perspectives in the regulatory mechanisms governing NMHC-IIA

functions in infection and physiological cellular processes. Further work should reveal whether NMHC-IIA-pTyr affects its motor activity, binding partners and/or the formation of actomyosin filaments.

ACKNOWLEDGEMENTS

pcDNA3-Src-KD was kindly provided by Sarah J. Parsons (University of Virginia). We are grateful to C. Portugal, R. Socodato and J.B. Relvas (Glial Cell Biology, IBMC) for their help with Src depletion experiments. This work was funded by the Fundo Europeu de Desenvolvimento Regional (FEDER) through the Operational Competitiveness Programme (COMPETE) and by National funds through FCT (Fundação para a Ciência e Tecnologia) under the projects (PTDC/BIA-BCM/100088/2008FCOMP-01-0124-FEDER-008860, ERANet-Pathogenomics LISTRESS ERA-PTG/0003/2010); Project “NORTE-07-0124-FEDER-000002-Host-Pathogen Interactions” co-funded by Programa Operacional Regional do Norte (ON.2 - O Novo Norte), under the Quadro de Referência Estratégico Nacional (QREN), through the FEDER and by FCT. We thank F. Carvalho for the critical reading of the manuscript and members of Cabanes group for helpful discussions. MTA and RC received FCT Doctoral Fellowships (BD/43352/2008 and BD/90607/2012). FSM was funded through an EMBO Long-term Post-doctoral Fellowship (EMBO ALTF 864-2012). SS was supported by Ciência 2008 and FCT Investigator programs (COMPETE, POPH, and FCT). We are grateful to Rui Appelberg for PhD co-supervision of MTA and RC.

REFERENCES

1. Allerberger, F., and Wagner, M. (2010) Listeriosis: a resurgent foodborne infection. *Clin Microbiology Infect.* **16**, 16-23
2. Lecuit, M. (2005) Understanding how *Listeria monocytogenes* targets and crosses host barriers. *Clin Microbiology Infect.* **11**, 430-436
3. Camejo, A., Carvalho, F., Reis, O., Leitao, E., Sousa, S., and Cabanes, D. (2011) The arsenal of virulence factors deployed by *Listeria monocytogenes* to promote its cell infection cycle. *Virulence* **2**, 379-394
4. Mengaud, J., Ohayon, H., Gounon, P., Mege, R. M., and Cossart, P. (1996) E-cadherin is the receptor for internalin, a surface protein required for entry of *L. monocytogenes* into epithelial cells. *Cell* **84**, 923-932

5. Shen, Y., Naujokas, M., Park, M., and Ireton, K. (2000) InIB-dependent internalization of *Listeria* is mediated by the Met receptor tyrosine kinase. *Cell* **103**, 501-510
6. Bierne, H., Gouin, E., Roux, P., Caroni, P., Yin, H. L., and Cossart, P. (2001) A role for cofilin and LIM kinase in *Listeria*-induced phagocytosis. *J. Cell Biol.* **155**, 101-112
7. Sousa, S., Cabanes, D., Bougneres, L., Lecuit, M., Sansonetti, P., Tran-Van-Nhieu, G., and Cossart, P. (2007) Src, cortactin and Arp2/3 complex are required for E-cadherin-mediated internalization of *Listeria* into cells. *Cell Microbiol* **9**, 2629-2643
8. Ireton, K., Payrastre, B., Chap, H., Ogawa, W., Sakaue, H., Kasuga, M., and Cossart, P. (1996) A role for phosphoinositide 3-kinase in bacterial invasion. *Science* **274**, 780-782
9. Ireton, K., Payrastre, B., and Cossart, P. (1999) The *Listeria monocytogenes* protein InlB is an agonist of mammalian phosphoinositide 3-kinase. *J. Biol. Chem.* **274**, 17025-17032
10. Kuhbacher, A., Dambournet, D., Echard, A., Cossart, P., and Pizarro-Cerda, J. (2012) Phosphatidylinositol 5-phosphatase oculocerebrorenal syndrome of Lowe protein (OCRL) controls actin dynamics during early steps of *Listeria monocytogenes* infection. *J. Biol. Chem.* **287**, 13128-13136
11. Bierne, H., Miki, H., Innocenti, M., Scita, G., Gertler, F. B., Takenawa, T., and Cossart, P. (2005) WASP-related proteins, Abi1 and Ena/VASP are required for *Listeria* invasion induced by the Met receptor. *J. Cell Sci.* **118**, 1537-1547
12. Seveau, S., Bierne, H., Giroux, S., Prevost, M. C., and Cossart, P. (2004) Role of lipid rafts in E-cadherin-- and HGF-R/Met--mediated entry of *Listeria monocytogenes* into host cells. *The Journal of cell biology* **166**, 743-753
13. Bonazzi, M., Vasudevan, L., Mallet, A., Sachse, M., Sartori, A., Prevost, M. C., Roberts, A., Taner, S. B., Wilbur, J. D., Brodsky, F. M., and Cossart, P. (2011) Clathrin phosphorylation is required for actin recruitment at sites of bacterial adhesion and internalization. *J. Cell Biol.* **195**, 525-536
14. Bonazzi, M., Veiga, E., Pizarro-Cerda, J., and Cossart, P. (2008) Successive post-translational modifications of E-cadherin are required for InlA-mediated internalization of *Listeria monocytogenes*. *Cell Microbiol* **10**, 2208-2222
15. Vicente-Manzanares, M., Ma, X., Adelstein, R. S., and Horwitz, A. R. (2009) Non-muscle myosin II takes centre stage in cell adhesion and migration. *Nat. Rev. Mol. Cell Biol* **10**, 778-790
16. Arii, J., Goto, H., Suenaga, T., Oyama, M., Kozuka-Hata, H., Imai, T., Minowa, A., Akashi, H., Arase, H., Kawaoka, Y., and Kawaguchi, Y. (2010) Non-muscle myosin IIA is a functional entry receptor for herpes simplex virus-1. *Nature* **467**, 859-862
17. Valiya Veetil, M., Sadagopan, S., Kerur, N., Chakraborty, S., and Chandran, B. (2010) Interaction of c-Cbl with myosin IIA regulates Bleb associated macropinocytosis of Kaposi's sarcoma-associated herpesvirus. *PLoS Pathog* **6**, e1001238
18. Hanisch, J., Kolm, R., Wozniczka, M., Bumann, D., Rottner, K., and Stradal, T. E. (2011) Activation of a RhoA/myosin II-dependent but Arp2/3 complex-independent pathway facilitates *Salmonella* invasion. *Cell Host Microbe* **9**, 273-285
19. Hybiske, K., and Stephens, R. S. (2007) Mechanisms of host cell exit by the intracellular bacterium *Chlamydia*. *Proc. Natl. Acad. Sci. U. S. A.* **104**, 11430-11435
20. Wei, Q., and Adelstein, R. S. (2000) Conditional expression of a truncated fragment of nonmuscle myosin II-A alters cell shape but not cytokinesis in HeLa cells. *Mol. Biol. Cell* **11**, 3617-3627
21. Reis, O., Sousa, S., Camejo, A., Villiers, V., Gouin, E., Cossart, P., and Cabanes, D. (2010) LapB, a novel *Listeria monocytogenes* LPXTG surface adhesin, required for entry into eukaryotic cells and virulence. *J Infect Dis.* **202**, 551-562
22. Campellone, K. G., Roe, A. J., Lobner-Olesen, A., Murphy, K. C., Magoun, L., Brady, M. J., Donohue-Rolfe, A., Tzipori, S., Gally, D. L., Leong, J. M., and Marinus, M. G. (2007) Increased adherence and actin pedestal formation by dam-deficient enterohaemorrhagic *Escherichia coli* O157:H7. *Mol. Microbiol.* **63**, 1468-1481

23. Osorio, H., and Reis, C. A. (2013) Mass spectrometry methods for studying glycosylation in cancer. *Methods Mol. Biol.* **1007**, 301-316
24. Isberg, R. R., and Falkow, S. (1985) A single genetic locus encoded by *Yersinia pseudotuberculosis* permits invasion of cultured animal cells by *Escherichia coli* K-12. *Nature* **317**, 262-264
25. Kirchner, M., and Higgins, D. E. (2008) Inhibition of ROCK activity allows InlF-mediated invasion and increased virulence of *Listeria monocytogenes*. *Mol. Microbiol.* **68**, 749-767
26. Wilson, L. K., Luttrell, D. K., Parsons, J. T., and Parsons, S. J. (1989) pp60c-src tyrosine kinase, myristylation, and modulatory domains are required for enhanced mitogenic responsiveness to epidermal growth factor seen in cells overexpressing c-src. *Mol. Cell. Biol.* **9**, 1536-1544
27. Straight, A. F., Cheung, A., Limouze, J., Chen, I., Westwood, N. J., Sellers, J. R., and Mitchison, T. J. (2003) Dissecting temporal and spatial control of cytokinesis with a myosin II Inhibitor. *Science* **299**, 1743-1747
28. Pizarro-Cerda, J., Kuhbacher, A., and Cossart, P. (2012) Entry of *Listeria monocytogenes* in Mammalian Epithelial Cells: An Updated View. *Cold Spring Harb Perspect Med* **2**, a010009
29. Alrutz, M. A., and Isberg, R. R. (1998) Involvement of focal adhesion kinase in invasin-mediated uptake. *Proc. Natl. Acad. Sci. U. S. A.* **95**, 13658-13663
30. Guo, A., Villen, J., Kornhauser, J., Lee, K. A., Stokes, M. P., Rikova, K., Possemato, A., Nardone, J., Innocenti, G., Wetzel, R., Wang, Y., MacNeill, J., Mitchell, J., Gygi, S. P., Rush, J., Polakiewicz, R. D., and Comb, M. J. (2008) Signaling networks assembled by oncogenic EGFR and c-Met. *Proc. Natl. Acad. Sci. U. S. A.* **105**, 692-697
31. Rikova, K., Guo, A., Zeng, Q., Possemato, A., Yu, J., Haack, H., Nardone, J., Lee, K., Reeves, C., Li, Y., Hu, Y., Tan, Z., Stokes, M., Sullivan, L., Mitchell, J., Wetzel, R., MacNeill, J., Ren, J. M., Yuan, J., Bakalarski, C. E., Villen, J., Kornhauser, J. M., Smith, B., Li, D., Zhou, X., Gygi, S. P., Gu, T. L., Polakiewicz, R. D., Rush, J., and Comb, M. J. (2007) Global survey of phosphotyrosine signaling identifies oncogenic kinases in lung cancer. *Cell* **131**, 1190-1203
32. Harney, D. F., Butler, R. K., and Edwards, R. J. (2005) Tyrosine phosphorylation of myosin heavy chain during skeletal muscle differentiation: an integrated bioinformatics approach. *Theor Biol Med Model.* **2**, 12
33. Dominguez, R., Freyzon, Y., Trybus, K. M., and Cohen, C. (1998) Crystal structure of a vertebrate smooth muscle myosin motor domain and its complex with the essential light chain: visualization of the pre-power stroke state. *Cell* **94**, 559-571
34. Barfod, E. T., Moore, A. L., Melnick, R. F., and Lidofsky, S. D. (2005) Src regulates distinct pathways for cell volume control through Vav and phospholipase Cgamma. *J. Biol. Chem.* **280**, 25548-25557
35. Barfod, E. T., Moore, A. L., Van de Graaf, B. G., and Lidofsky, S. D. (2011) Myosin light chain kinase and Src control membrane dynamics in volume recovery from cell swelling. *Mol. Biol. Cell* **22**, 634-650
36. Chakraborty, S., Veettil, M. V., Bottero, V., and Chandran, B. (2012) Kaposi's sarcoma-associated herpesvirus interacts with EphrinA2 receptor to amplify signaling essential for productive infection. *Proc. Natl. Acad. Sci. U. S. A.* **109**, E1163-1172
37. Wasylanka, J. A., Bakowski, M. A., Szeto, J., Ohlson, M. B., Trimble, W. S., Miller, S. I., and Brumell, J. H. (2008) Role for myosin II in regulating positioning of Salmonella-containing vacuoles and intracellular replication. *Infect. Immun.* **76**, 2722-2735
38. Rajabian, T., Gavicherla, B., Heisig, M., Muller-Altroch, S., Goebel, W., Gray-Owen, S. D., and Ireton, K. (2009) The bacterial virulence factor InlC perturbs apical cell junctions and promotes cell-to-cell spread of *Listeria*. *Nat. Cell Biol.* **11**, 1212-1218
39. Mostowy, S., Bonazzi, M., Hamon, M. A., Tham, T. N., Mallet, A., Lelek, M., Gouin, E., Demangel, C., Brosch, R., Zimmer, C., Sartori, A., Kinoshita, M., Lecuit, M., and Cossart, P. (2010) Entrapment of intracytosolic bacteria by septin cage-like structures. *Cell Host Microbe* **8**, 433-444

40. Odendall, C., Rolhion, N., Forster, A., Poh, J., Lamont, D. J., Liu, M., Freemont, P. S., Catling, A. D., and Holden, D. W. (2012) The *Salmonella* kinase SteC targets the MAP kinase MEK to regulate the host actin cytoskeleton. *Cell Host Microbe* **12**, 657-668
41. Cai, Y., Rossier, O., Gauthier, N. C., Biais, N., Fardin, M. A., Zhang, X., Miller, L. W., Ladoux, B., Cornish, V. W., and Sheetz, M. P. (2010) Cytoskeletal coherence requires myosin-IIA contractility. *J. Cell Sci.* **123**, 413-423
42. Cai, Y., and Sheetz, M. P. (2009) Force propagation across cells: mechanical coherence of dynamic cytoskeletons. *Curr. Opin. Cell Biol.* **21**, 47-50
43. Veiga, E., and Cossart, P. (2006) The role of clathrin-dependent endocytosis in bacterial internalization. *Trends Cell Biol.* **16**, 499-504
44. Giannone, G., Dubin-Thaler, B. J., Rossier, O., Cai, Y., Chaga, O., Jiang, G., Beaver, W., Dobereiner, H. G., Freund, Y., Borisy, G., and Sheetz, M. P. (2007) Lamellipodial actin mechanically links myosin activity with adhesion-site formation. *Cell* **128**, 561-575
45. Cai, Y., Biais, N., Giannone, G., Tanase, M., Jiang, G., Hofman, J. M., Wiggins, C. H., Silberzan, P., Buguin, A., Ladoux, B., and Sheetz, M. P. (2006) Nonmuscle myosin IIA-dependent force inhibits cell spreading and drives F-actin flow. *Biophys. J.* **91**, 3907-3920
46. Choi, C. K., Vicente-Manzanares, M., Zareno, J., Whitmore, L. A., Mogilner, A., and Horwitz, A. R. (2008) Actin and alpha-actinin orchestrate the assembly and maturation of nascent adhesions in a myosin II motor-independent manner. *Nat. Cell Biol.* **10**, 1039-1050
47. Smutny, M., Cox, H. L., Leerberg, J. M., Kovacs, E. M., Conti, M. A., Ferguson, C., Hamilton, N. A., Parton, R. G., Adelstein, R. S., and Yap, A. S. (2010) Myosin II isoforms identify distinct functional modules that support integrity of the epithelial zonula adherens. *Nat. Cell Biol.* **12**, 696-702
48. Bertet, C., Sulak, L., and Lecuit, T. (2004) Myosin-dependent junction remodelling controls planar cell intercalation and axis elongation. *Nature* **429**, 667-671
49. McLachlan, R. W., Kraemer, A., Helwani, F. M., Kovacs, E. M., and Yap, A. S. (2007) E-cadherin adhesion activates c-Src signaling at cell-cell contacts. *Mol. Biol. Cell* **18**, 3214-3223
50. Organ, S. L., and Tsao, M. S. (2011) An overview of the c-MET signaling pathway. *Ther Adv in Med Oncol.* **3**, S7-S19
51. Chandran, B. (2010) Early events in Kaposi's sarcoma-associated herpesvirus infection of target cells. *J. Virol.* **84**, 2188-2199
52. Veiga, E., and Cossart, P. (2005) *Listeria* hijacks the clathrin-dependent endocytic machinery to invade mammalian cells. *Nat. Cell Biol.* **7**, 894-900
53. Isberg, R. R., and Leong, J. M. (1990) Multiple beta 1 chain integrins are receptors for invasins, a protein that promotes bacterial penetration into mammalian cells. *Cell* **60**, 861-871
54. Rivera Rosado, L. A., Horn, T. A., McGrath, S. C., Cotter, R. J., and Yang, J. T. (2011) Association between alpha4 integrin cytoplasmic tail and non-muscle myosin IIA regulates cell migration. *J. Cell Sci.* **124**, 483-492
55. Destaing, O., Block, M. R., Planus, E., and Albiges-Rizo, C. (2011) Invadosome regulation by adhesion signaling. *Curr. Opin. Cell Biol.* **23**, 597-606
56. Bruce-Staskal, P. J., Weidow, C. L., Gibson, J. J., and Bouton, A. H. (2002) Cas, Fak and Pyk2 function in diverse signaling cascades to promote *Yersinia* uptake. *J. Cell Sci.* **115**, 2689-2700

FIGURE LEGENDS

Figure 1. NMHC-IIA is tyrosine-phosphorylated in response to human bacterial pathogens. (A) Silver-stained acrylamide gel showing the tyrosine phosphorylation profiles of non-infected (NI) and *Lm*-infected HeLa cells, for the indicated periods of time. Total tyrosine-phosphorylated proteins were immunoprecipitated with an anti-pTyr antibody. Molecular weight standards are indicated. Arrow shows a

protein band with increased intensity over the time of infection and identified by mass spectrometry analysis as NMHC-IIA. (B) HeLa and Caco-2 cells were left non-infected (NI) or incubated with *Lm* and harvested at indicated time points post-infection (p.i.). Tyrosine-phosphorylated proteins were immunoprecipitated (IP: pTyr) from whole cell lysates (WCL) and NMHC-IIA was detected by immunoblot (NMHC-IIA) in IP fractions and WCL. Detection of actin protein levels served as loading control. Bottom panels show quantifications of NMHC-IIA signals from at least 3 independent experiments in WCL and IP fractions of NI and *Lm*-infected HeLa (60 min p.i.) and Caco-2 (20 min p.i.) cells. (C) HeLa cells were left NI or incubated with either *Lm*, *L. innocua* (*Li*) (top panels), *E. coli* DH5 α (*Ec*) or latex beads (bottom panels). Tyrosine-phosphorylated proteins were immunoprecipitated from WCL recovered at different time points and NMHC-IIA was analyzed by immunoblot in IP fractions and WCL. (D) HeLa cells were left NI or incubated, for 4 h, with pathogenic *E. coli* (EPEC and EHEC) and *E. coli* K12 expressing a functional (*inv*) or mutated variant (Δ *inv*) of *Y. pseudotuberculosis* invasin. Cells were also incubated with *Lm* for 1 and 4 h (right panel). Tyrosine-phosphorylated proteins were immunoprecipitated and NMHC-IIA detected by immunoblot in IP fractions and WCL. Quantifications of NMHC-IIA signals for each IP fraction related to WCL are indicated (ratio). Values represent the mean of three independent experiments. (E) NMHC-IIA was immunoprecipitated (IP: NMHC-IIA) from WCL of NI and *Lm*-infected (Inf, 60 min) HeLa cells. Tyrosine-phosphorylated proteins (pTyr) and NMHC-IIA were detected in immunoprecipitates. As control, NMHC-IIA and actin were also detected in WCL.

Figure 2. The activity of Src kinase is required for NMHC-IIA tyrosine phosphorylation upon *Lm* cellular infection. (A) HeLa cells pre-treated with PP1 (10 μ M) or Y-27632 (50 μ M) during 30 min, were left NI or incubated with *Lm* for 1 h (Inf) in the presence of the same concentrations of drugs. Non-treated (NT) HeLa cells were used as control. (B) HeLa cells non-transfected (NT), transfected with a control empty plasmid (Ctr) or with a Src kinase dead (Src-KD)-encoding plasmid. (C) HeLa cells stably expressing an shRNA control (sh Ctr) or a specific shRNA targeting Src expression (sh Src). Cells in B and C were left NI or incubated with *Lm* for 1 h (Inf). In A, B and C, total tyrosine-phosphorylated proteins were immunoprecipitated and NMHC-IIA was detected by immunoblot in IP fractions and WCL. Detection of actin levels served as loading control. Src protein levels were also confirmed by immunoblot. (D) Efficiency of Src depletion in sh Src HeLa cells was assessed by immunoblot using actin protein detection as loading control (left panel) and by qRT-PCR (right panel). Src mRNA expression is represented relative to the expression of control HPRT1. In sh Ctr cells, the relative expression was arbitrarily fixed to 1.

Figure 3. NMHC-IIA tyrosine residue in position 158 is phosphorylated in response to *Lm* infection. (A) Schematic representation of NMHC-IIA showing the distribution of tyrosine residues (red bars). Tyrosine residues in position 158 (Y158) and 190 (Y190) are highlighted. ATP-binding site, motor and tail domains are indicated. (B) *In silico* predictions obtained from NetPhos 2.0 and NetPhosK servers, for tyrosine phosphorylation potential (score) and putative kinase involved. The position and amino acid environment of tyrosine residues showing a phosphorylation potential above the threshold (score >0.5) are indicated. (C) HeLa cells expressing the wild type GFP-NMHC-IIA (WT) and the mutants GFP-NMHC-IIA-Y158F (Y158F) or GFP-NMHC-IIA-Y190F (Y190F) were left NI or incubated with *Lm* for 1 h (Inf). NMHC-IIA was detected by immunoblot in anti-pTyr immunoprecipitates and WCL. Detection of GFP indicates similar expression levels of NMHC-IIA constructs and actin levels served as loading control. (D) HeLa cells were left NI or incubated with *Lm* for 1 h (Inf). Total cell extracts were used in immunoblot using an antibody raised against NMHC-IIA-pY158. Total levels of NMHC-IIA were detected using an anti-NMHC-IIA antibody and α -tubulin levels were used as loading control. Bottom panel show quantification of NMHC-IIA-pY158 signals from 3 independent experiments in NI and *Lm*-infected HeLa cells. (E) Mass spectra from NMHC-IIA acquired after phosphopeptide enrichment from NI and Inf HeLa cells. Two peak clusters marked as I (monoisotopic peak at m/z 3025.37 [M-H]⁺) and II (monoisotopic peak at m/z 3041.36 [M-H]⁺ with oxidized methionine) were detected. The corresponding NMHC-IIA peptide (aa 142 to 165) is indicated and Y158 highlighted. The area of the clusters in NI and Inf

conditions is indicated between parentheses. (F) Anti-GFP IP fractions obtained from WCL of HEK293 cells expressing either GFP-NMHC-IIA-WT (WT) or GFP-NMHC-IIA-Y158F (Y158F) were used in *in vitro* Src kinase assays. A synthetic peptide was used as positive control (Ctr). Incorporation of radiolabeled γ -³²P-ATP was measured in CPM (counts per minute) for each condition. Results are representative of two independent experiments. (G) Comparative analysis of the NMHC-IIA amino acid sequence from different species, focused in the region encompassing the tyrosine on position 158.

Figure 4. *Lm* intracellular levels increased upon inhibition of NMHC-IIA activity. (A) Levels of intracellular *Lm* were assessed by gentamicin protection assay and CFU counting, in HeLa and Caco-2 cells treated with 10 or 100 μ M blebbistatin (Blebb). Graph shows the fold-increase of intracellular *Lm* determined as the ratio of intracellular bacteria in cells treated with the active *versus* the inactive enantiomer of blebbistatin. (B) Single confocal sections of HeLa cells infected with *Lm* in the presence of DMSO (control) or 50 μ M active Blebbistatin. Infected cells were immunolabelled for NMHC-IIA (green) and *Lm* (blue) and stained for actin (red). (C) Immunofluorescence scoring of DMSO- and active Blebbistatin-treated HeLa cells associated to *Lm* and showing *Lm*-associated actin foci. Results are means \pm SD from three independent experiments, each done in duplicate. Statistically significant differences are indicated: * $p < 0.05$.

Figure 5. Depletion of NMHC-IIA facilitated *Lm* cellular infection. (A) Intracellular levels of *Lm* assessed by gentamicin protection assay in HeLa cells non-transfected (NT) or transfected with either control siRNA (Ctr) or NMHC-IIA-specific siRNAs (si#1 and si#2). Efficiency of NMHC-IIA knockdown was assessed by immunoblot and quantified. Indicated values (Normalized expression) are relative to actin and NMHC-IIA expression levels in NT cells. (B) Percentage of control (Ctr) or NMHC-IIA-depleted cells (IIA-si#1) associated to *Lm* and showing *Lm*-associated actin foci, evaluated by immunofluorescence scoring. (C) Number of bacteria and actin foci per cell in control and NMHC-IIA-depleted conditions. (D) Depletion of NMHC-IIA does not affect the expression of NMHC-IIB. NMHC-IIB expression levels were evaluated by immunoblot in NMHC-IIA-depleted (IIA-si#1) as compared to control (NT and Ctr) cells. Actin was used as loading control. (E) Intracellular levels of *Lm* were assessed by gentamicin protection assay in HeLa cells transfected with either control siRNA (Ctr) or NMHC-IIB-specific siRNA (IIB-si). Efficiency of NMHC-IIB knockdown was assessed by immunoblot using actin protein detection as loading control. (F) Expression of NMHC-IIA was restored in si#2-depleted cells through the expression of a siRNA-resistant GFP-NMHC-IIA (NMHC-IIA-siRes). Intracellular levels of *Lm* assessed by gentamicin protection assay in HeLa cells expressing different levels of NMHC-IIA are shown. Non-treated and NMHC-IIA-depleted cells expressing a wild type GFP-NMHC-IIA (NMHC-IIA-WT) were used as controls. Endogenous NMHC-IIA silencing and GFP-NMHC-IIA expression was evaluated by immunoblot. Detection of actin levels served as loading control. (G) Western blot showing expression levels of endogenous (anti-NMHC-IIA, M8064, Sigma-Aldrich) and ectopically expressed NMHC-IIA (anti-GFP, B2, Santa Cruz Biotech) in HeLa cells transfected either with GFP-NMHC-IIA-WT or GFP-NMHC-IIA-siRes expression vectors. (H) Intracellular levels of *L. innocua* expressing *inlB* (*Li-inlB*), *E. coli* K12 expressing the invasin (K12-*inv*) and *Y. pseudotuberculosis* (Yp) were assessed by gentamicin protection assay in HeLa cells transfected with either control siRNA (Ctr) or NMHC-IIA-specific siRNA (IIA-si#1). In panels A and F, the number of intracellular *Lm* in NT cells was normalized to 100% and those in siRNA-transfected cells were expressed as relative values to NT cells. In panels E and H, numbers of intracellular bacteria were normalized to 100% in Ctr cells and expressed as relative values in the other conditions. Results shown in panels A, B, C, E, F and H are means \pm SEM of at least three independent experiments, each done in triplicate. Statistically significant differences are indicated: * $p < 0.05$, ** $p < 0.01$ and *** $p < 0.001$.

Figure 6. NMHC-IIA phosphorylation in tyrosine 158 is required to limit *Lm* cellular infection. (A and B) Intracellular levels of *Lm* assessed by gentamicin protection assays in the presence of 10 μ M PP1

(A) or in HeLa cells expressing Src-KD (B). (C) Levels of intracellular K12-*inv* were assessed by gentamicin protection assay in HeLa cells treated with 10 μ M of PP1. (D) Intracellular levels of *Lm* were assessed by gentamicin protection assays in HeLa and COS-7 cells expressing either GFP-NMHC-IIA-WT (WT) or GFP-NMHC-IIA-Y158F (Y158F). Results shown in panels A, B, C and D are means \pm SEM of three independent experiments, each done in triplicate. Numbers of intracellular bacteria were normalized to 100% in control cells and expressed as relative values in the other experimental conditions. Statistically significant differences are indicated: * $p < 0.05$, ** $p < 0.01$. (E) Single confocal section of COS-7 cells ectopically expressing either GFP-NMHC-IIA-WT or Y158F variants incubated with *Lm* for 1 h and stained for actin (phalloidin, red) and DNA (DAPI, blue) (scale bar 10 μ m).

Table 1. List of bacterial strains used in this study and the corresponding growth conditions.

Bacterial strains	Growth Media	T (°C)
<i>L. monocytogenes</i> (EGDe)	BHI (Difco Laboratories)	37
<i>L. innocua</i> (CLIP 11262)	BHI	37
<i>L. innocua-inlB</i>	BHI Erythromycin 5µg/ml	37
<i>E. coli</i> DH5α	LB (Difco Laboratories)	37
EPEC	LB Ampicilin 100 µg/ml (Amp100)	37
EHEC	LB	37
<i>E. coli</i> K12- <i>inv</i>	LB Amp100	37
<i>E. coli</i> K12- <i>Δinv</i>	LB Amp100	37
<i>Y. pseudotuberculosis</i>	LB Amp100	26

Table 2. List of plasmids used in this study.

Plasmid	Description	Source
GFP-NMHCIIA-WT	pEGFP-C3:CMV-GFP-NMHC IIA	Addgene (#11347)
GFP-NMHCIIA-Y158F	pEGFP-C3:CMV-GFP-NMHC IIA (Y158F)	This study
GFP-NMHCIIA-Y190F	pEGFP-C3:CMV-GFP-NMHC IIA (Y190F)	This study
GFP-NMHCIIA-WT-siRes	pEGFP-C3:CMV-GFP-NMHC IIA siRNA resistant	This study
Src-KD	pcDNA3-Src Kinase Dead (A430V)	Sarah J. Parsons, Univ. of Virginia

Table 3. List of antibodies used in this study.

Antigen	Species	Applications	Reference	Source
Phosphotyrosine	Mouse	IP (1:300) WB (1:1000)	4G10, 05-321	Millipore
Phosphotyrosine	Mouse	WB (1:1000)	PY20, P4110	Sigma-Aldrich
Actin	Mouse	WB (1:5000)	AC-15, A5441	Sigma-Aldrich
NMHC-IIA	Mouse	IF (1:1000)	ab55456	Abcam
GFP	Mouse	IP (1:100) WB (1:500)	B2, sc-9996	Santa Cruz Biotechnology
NMHC-IIA pY158	Rabbit	WB (1:500)	AP3775a	Abgent
<i>Listeria</i>	Rabbit	IF (1:200)	ab35132	Abcam
NMHC-IIA	Rabbit	IP (1:100) WB (1:5000)	M8064	Sigma-Aldrich
c-Src	Rabbit	WB (1:500)	GD11, 05-184	Millipore
c-Src	Rabbit	WB (1:1000)	ab109381	Abcam
NMHC-IIB	Rabbit	WB (1:1000)	M7939	Sigma-Aldrich
Anti-rabbit or anti-mouse HRP	Goat	WB	BI2413C BI2407	PARIS
Anti-rabbit or anti-mouse Alexa Fluor 488	Goat	IF	A11034 A11001	Invitrogen
Anti-rabbit or anti-mouse Cy3	Goat	IF	111-165-144 115-165-146	Jackson ImmunoResearch
Anti-rabbit or anti-mouse Cy5	Goat	IF	111-175-144 115-175-146	Jackson ImmunoResearch

Table 4. Sequences of siRNA duplexes, shRNAs and primers used in this study.

siRNA duplexes			
Name		Oligo Sequence (5'-3')	Source
NMHCIIA-si#1 (Pool of 3 siRNAs)	A	Sense: CAUCUACUCUGAAGAGAUUtt	Santa Cruz Biotechnology (#sc-61120)
		Antisense: AAUCUCUUCAGAGUAGAUGtt	
	B	Sense: GAAGAUCAAUCCAUCUUGUtt	
		Antisense: ACAAGAUGGAUUGAUCUUCtt	
	C	Sense: CCAAAGAGAACGAGAAGAAtt	
		Antisense: UUCUUCUCGUUUCUUIUGGtt	
NMHCIIA-si#2		Sense: GAAGAUCAAUCCAUCUUGUtt	Santa Cruz Biotechnology (#sc-61120B)
NMHCIIB-si		Antisense: ACAAGAUGGAUUGAUCUUCtt	Sigma-Aldrich (#00072460)
		Sense: GCAAUACAGUGGGACAGUUtt	
		Antisense: AACUGUCCACUGUAUUGCtt	
shRNAs Sequence (5'-3') and Source			
Src	CCGGGTGGCTTACTACTCCAAACATCTCGAGATGTTTGGAGTAGTAAGCCACTTTTT Sigma-Aldrich (TRCN0000023597)		
Control	CCGGGCGCGATAGCGCTAATAATTTCTCGAGAAATTATTAGCGCTATCGCGCTTTTT Sigma-Aldrich (SHC016)		
Primers sequences (5'-3')			
NMHC-IIA-Y158F	Fw:	CTATGCCATCACAGACACCGCCTTCAGGAGTATGATGCAAGAC	
	Rev:	GTCTTGCAATCATACTCCTGAAGGCGGTGTCTGTGATGGCATAG	
NMHC-IIA-Y190F	Fw:	CACCAAGAAGGTCATCCAGTTCTGGCGTACGTGGCGTCTCG	
	Rev:	CGAGGACGCCACGTACGCCAGAACTGGATGACCTTCTTGGTG	
NMHC-IIA-WT-siRes	Fw:	GATGCAAGACCGGAGAGGATCAATCCATACTGTGCACTGGTGAATC	
	Rev:	GATTCAACAGTGCACAGTATGGATTGATCCTCTCGGTCTTGCATC	
c-Src	Fw:	CTGTTCCGAGGCTTCAACTC	
	Rev:	CCACCACTCTCCCTCTGTGT	
HPRT1	Fw:	GGCGTCGTGATTAGTAGTG	
	Rev:	CACCCTTTCCAAATCCTCAG	

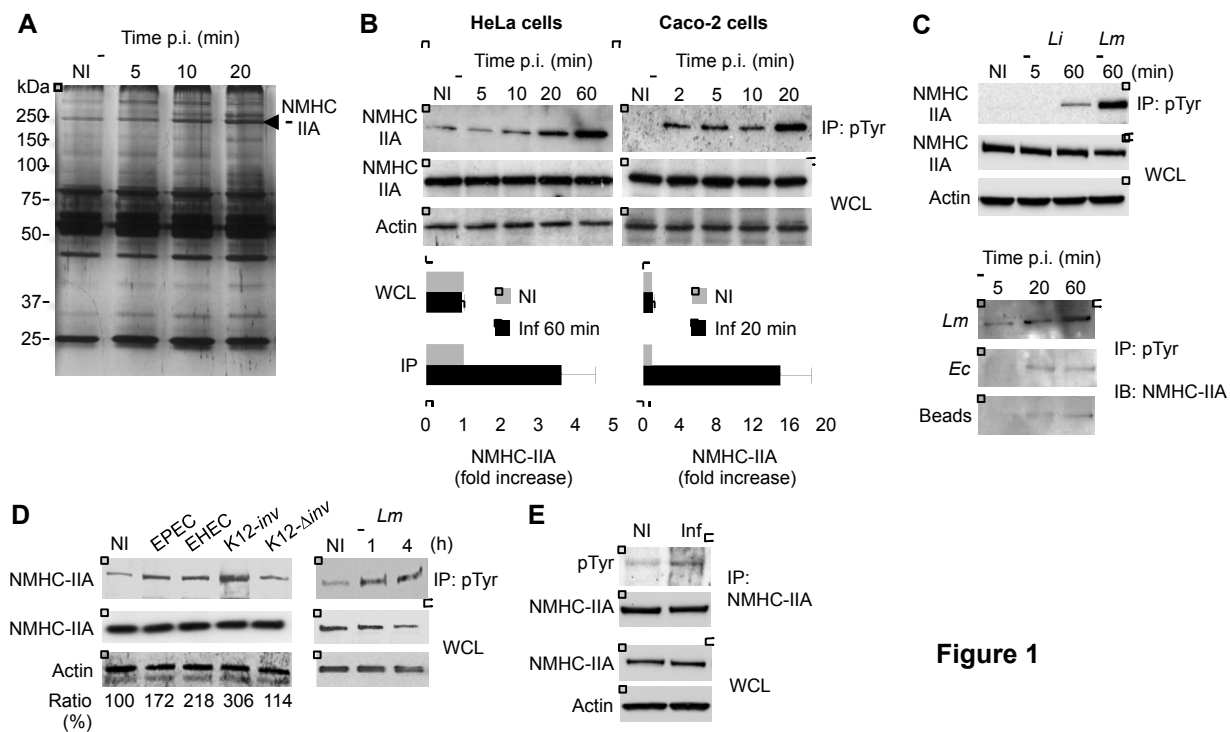


Figure 1

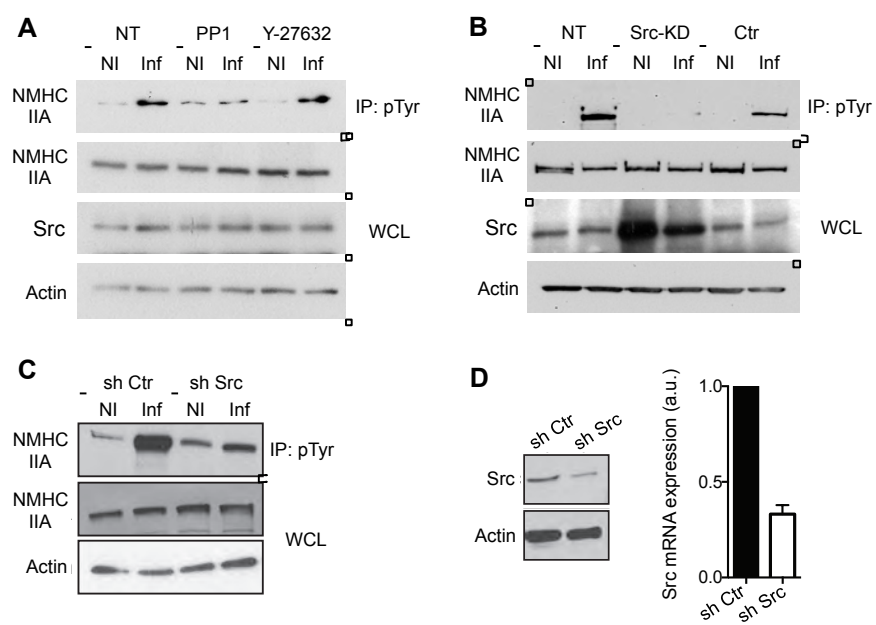


Figure 2

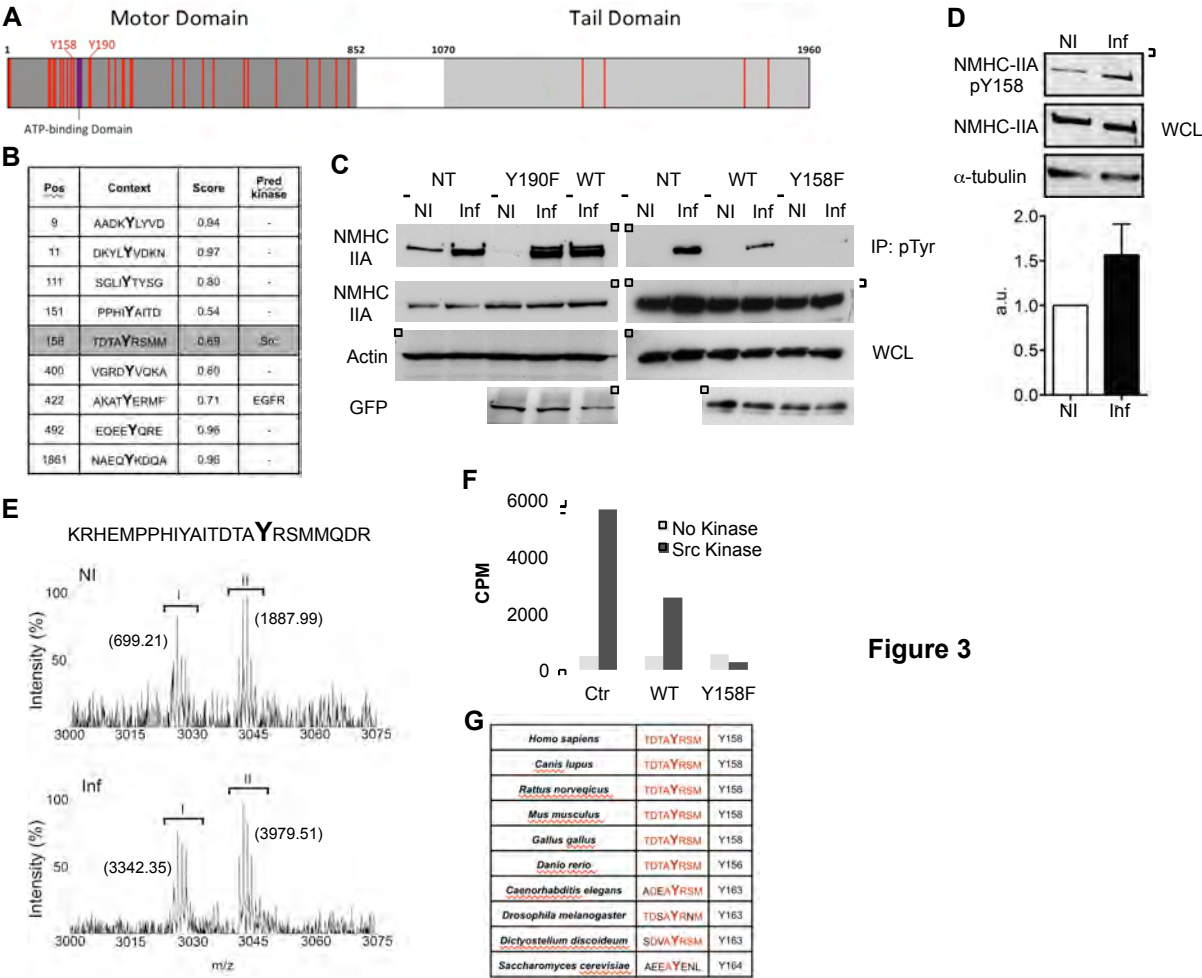


Figure 3

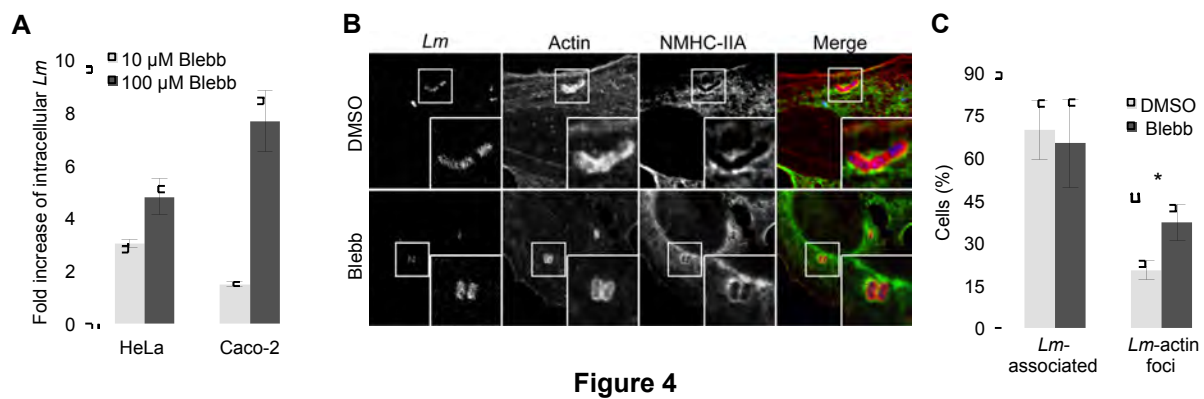


Figure 4

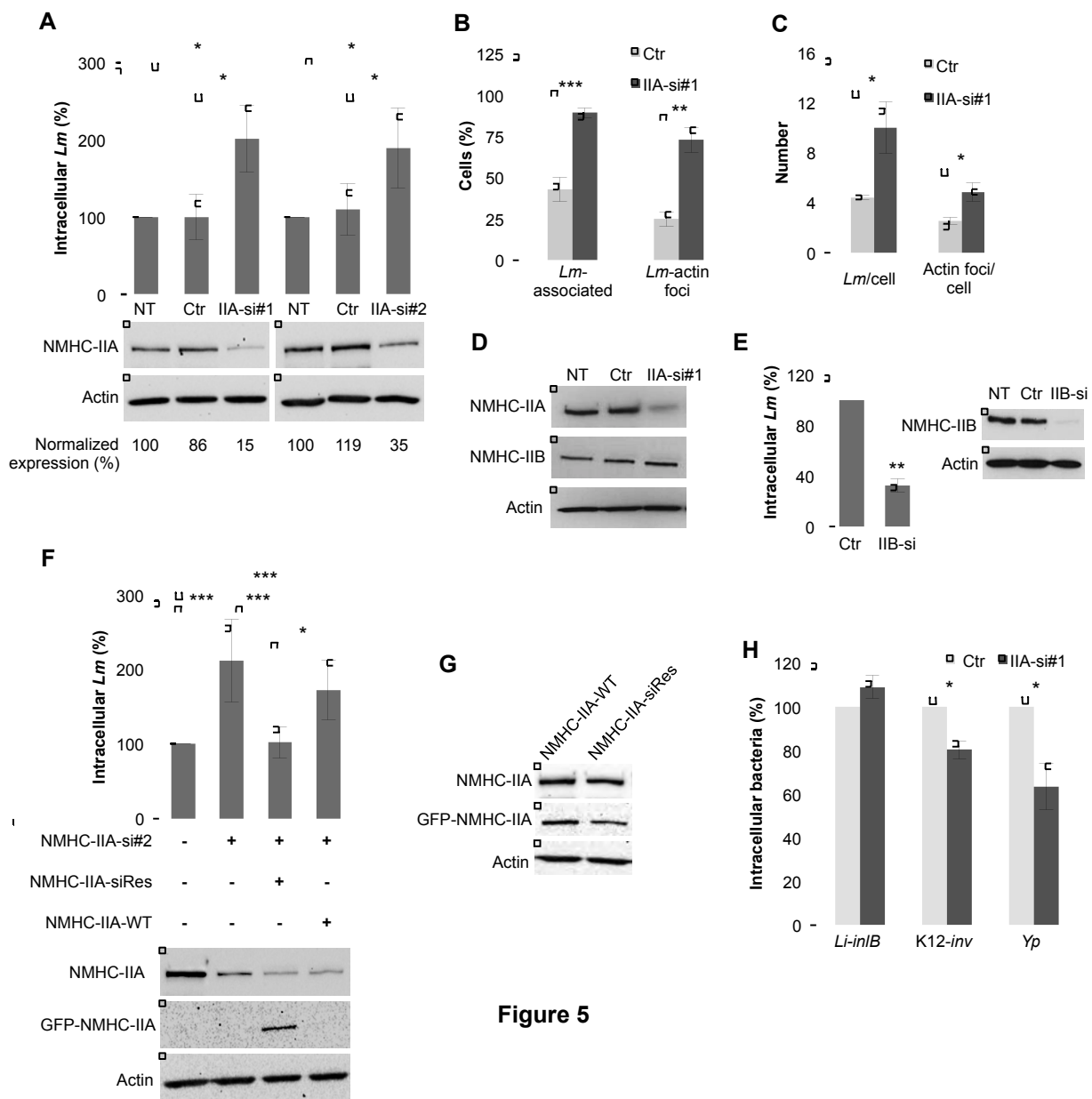


Figure 5

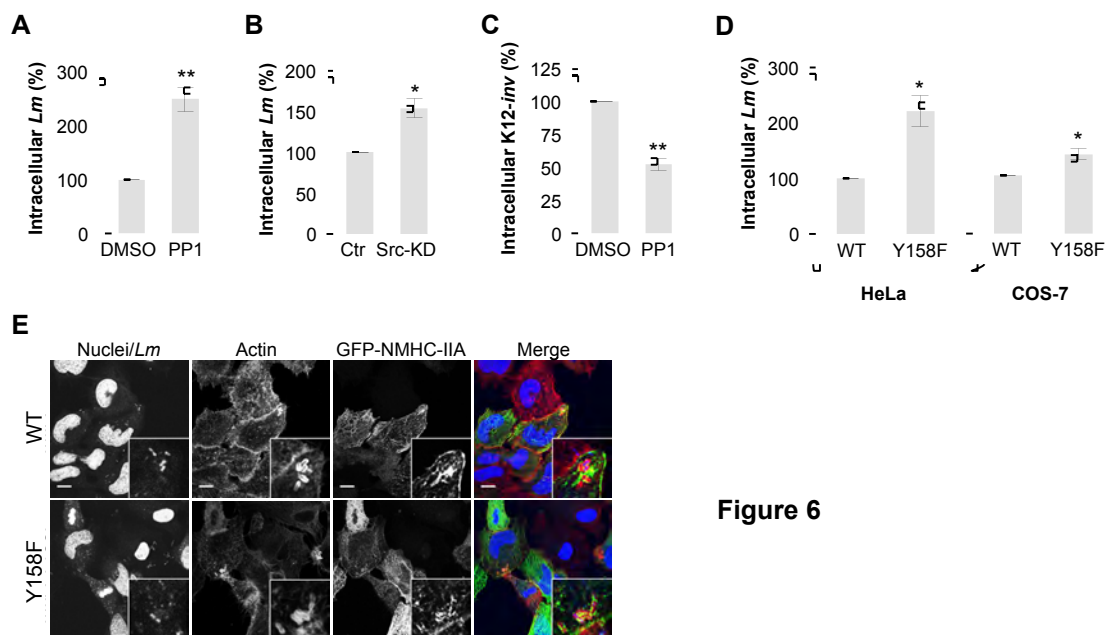


Figure 6